JACS Au
AN OPEN ACCESS JOURNAL OF THE AMERICAN CHEMICAL SOCIETY

pubs.acs.org/jacsau

Article

Transformation of Bulk Pd to Pd Cations in Small-Pore CHA Zeolites Facilitated by NO

Shunsaku Yasumura, Hajime Ide, Taihei Ueda, Yuan Jing, Chong Liu, Kenichi Kon, Takashi Toyao, Zen Maeno,* and Ken-ichi Shimizu*

Cite This: *JACS Au* 2021, 1, 201−211

Read Online

ACCESS | Metrics & More | Article Recommendations | Supporting Information

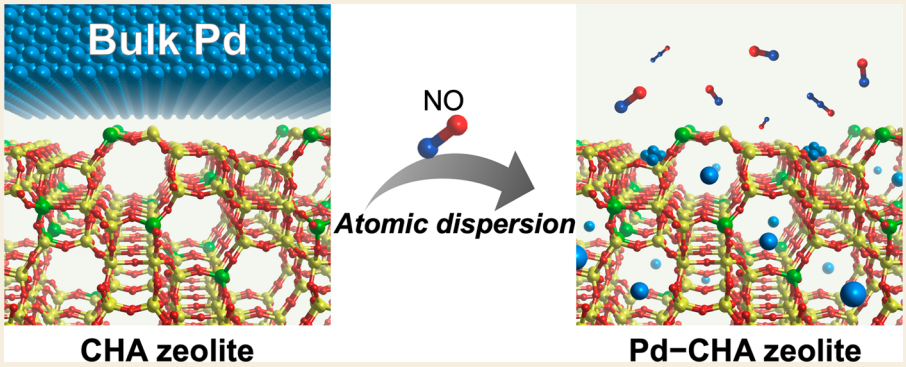

ABSTRACT: Atomic dispersion of metal species has attracted attention as a unique phenomenon that affects adsorption properties and catalytic activities and that can be used to design so-called single atom materials. In this work, we describe atomic dispersion of bulk Pd into small pores of CHA zeolites. Under 4% NO flow at 600 °C, bulk Pd metal on the outside of CHA zeolites effectively disperses, affording Pd^{2+} cations on Al sites with concomitant formation of N_2O, as revealed by microscopic and spectroscopic characterizations combined with mass spectroscopy. In the present method, even commercially available submicrosized Pd black can be used as a Pd source, and importantly, 4.1 wt % of atomic Pd^{2+} cations, which is the highest loading amount reported so far, can be introduced into CHA zeolites. The structural evolution of bulk Pd metal is also investigated by *in situ* X-ray absorption spectroscopy (XAS) and diffuse reflectance infrared Fourier transform spectroscopy (DRIFTS), as well as *ab initio* thermodynamic analysis using density functional theory (DFT) calculations.

KEYWORDS: *atomic dispersion, small-pore zeolites, palladium, in situ spectroscopy, ab initio thermodynamics*

1. INTRODUCTION

Supported metal species have been widely utilized as heterogeneous catalysts and adsorbers.[1−4] The morphology and oxidation state of immobilized metal species dynamically change with temperature and atmosphere.[5−20] Generally, exposure to high temperature induces aggregation of metal species to form larger particles via particle coalescence and atomic ripening. Particle coalescence involves temperature-induced movement of metal nanoparticles, while atomic ripening occurs via movement of atomic species on supports or in vapor phase. As an opposite phenomenon, atomic dispersion of metal species occurs when mobile atomic species are trapped by supports.[21−39] Several microscopic and spectroscopic studies on atomic dispersion have appeared recently, investigating structural evolution under various reaction conditions and their effects on catalytic and adsorption properties.[28,33−38] Atomic dispersion also has the potential to be applied to atomically dispersed materials as well as catalyst regeneration processes, and several examples have appeared.[23−25,29−31]

Aluminosilicate zeolites are promising oxide supports that anchor atomic metal species as cations due to their cation exchange abilities, as well as ubiquitousness of constituent elements (Si, Al, O) with commercial availability. In the case of divalent cations, such as Pd^{2+}, paired Al sites in three-dimensional zeolite frameworks serve as anchoring sites, stabilizing through electrostatic interactions. Among them, eight-membered ring zeolites, such as CHA, have high potential to suppress aggregation of metal cations under reaction conditions because of their small pore sizes (3.8 Å ×

Received: December 14, 2020
Published: January 13, 2021

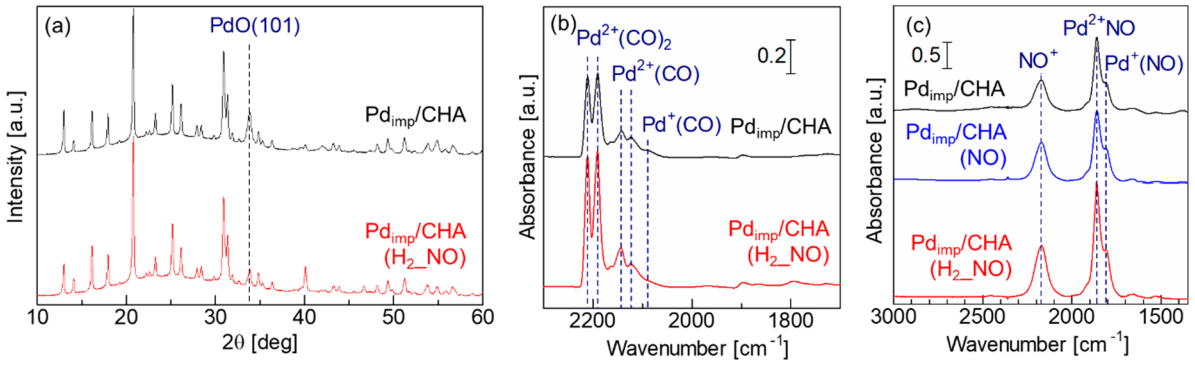

Figure 1. (a) XRD patterns and FTIR spectroscopy of (b) CO and (c) NO adsorption experiments for a series of Pd_{imp}/CHA. The CO adsorption experiment was conducted at room temperature under 0.1% CO/He flow, followed by a He purge, while the NO adsorption experiment was investigated at 100 °C under 0.1% NO/He flow. Prior to adsorption experiments, the sample was treated by 10% O_2/He to remove NO adsorbed during atomic dispersion. Detailed procedures are described in the SI.

3.8 Å) and superior stability toward hydrothermal conditions compared to medium- and large-pore zeolites.[40−44] Despite the fact that several metal-exchanged CHA zeolites, such as Cu-CHA, can be synthesized by conventional aqueous-phase ion exchange methods, loading Pd cations into CHA zeolites is difficult owing to strong water solvation of cations, which are too bulky to access the small pores. For example, Szanyi and co-workers loaded Pd cations into several zeolites via ion exchange in aqueous solution for use as passive NO_x adsorbers (PNAs), where isolated Pd cations are responsible for NO adsorption and aggregated PdO particles are ineffective.[45−47] Very small amounts of Pd (1.4%) were exchanged with cations in CHA in aqueous solution at Pd loading amounts of 0.5 wt %, while almost all the Pd (ca. 75%) was immobilized at ion-exchange sites in BEA and ZSM-5 under similar Pd loading amounts and Si/Al ratios of zeolites.[48] Kim and co-workers prepared Pd-modified CHA by incipient wetness impregnation and examined hydrothermal aging treatments at 700−750 °C to increase the number of active Pd cations for NO adsorption.[38] However, bulk PdO was the main Pd species, even after treatment, as confirmed by X-ray diffraction (XRD) and X-ray absorption spectroscopy (XAS) measurements. Although Pd cation loading (1−3.5 wt %) has been recently achieved via a modified aqueous-phase ion exchange method by the group of Szanyi,[40] the development of effective methods to load Pd cations in small-pore zeolites still needs to be addressed.

In this study, we describe atomic dispersion of bulk Pd into CHA zeolites for solid-state synthesis of Pd-exchanged CHA. Bulk Pd metal outside the CHA zeolites is transformed into Pd^{2+} cations on zeolite anionic sites under NO flow at 600 °C. Preparation of Pd-exchanged CHA zeolites from commercially available Pd black and CHA zeolites was also achieved.

Although redispersion of aggregated metal clusters in medium- and large-pore zeolites[21,22,30,32,37,39] and the transport of metal cations/nanoparticles from the outside of CHA zeolites have been reported,[25,49] atomic dispersion of bulk Pd from outside into small-pore zeolites has not yet been reported. Microscopic (scanning electron microscopy (SEM) and scanning transmission electron microscopy (STEM)) and spectroscopic (XRD, XAS, and Fourier transform infrared (FTIR)) characterizations revealed that atomic Pd^{2+} cations were mainly formed, and the loading amount of Pd^{2+} cations reached ca. 4 wt %. *In situ* spectroscopic studies (XAS and diffuse reflectance infrared Fourier transform spectroscopy (DRIFTS)) and *ab initio* thermodynamics analysis using density functional theory (DFT) were also conducted to gain insight into atomic dispersion of bulk Pd in CHA zeolites. Furthermore, a plausible mechanism was theoretically studied to discuss the reason for the necessity of high reaction temperature.

2. EXPERIMENTAL SECTION

Pd-modified CHA zeolites were prepared through impregnation of $Pd(NH_3)_2(NO_3)_2$ on CHA (NH_4-type, Tosoh, SiO_2/Al_2O_3 = 13.7), followed by calcination in 10% O_2/He at 600 °C (denoted as Pd_{imp}/CHA). Subsequently, Pd_{imp}/CHA was treated by 0.5% H_2/He flow at 500 °C and then exposed to 4% NO/He flow at 600 °C to load Pd^{2+} cations by atomic dispersion (denoted as Pd_{imp}/CHA(H_2_NO)). The total amount of Pd was determined based on the amounts of Pd precursor and CHA zeolites. The atomic dispersion reaction was conducted using a self-supported pellet in a flow-type quartz cell connected to a flow reaction system. XRD, SEM, STEM, and *ex situ* XAS were conducted after exposing the samples to air. CO, NO, and NH_3 adsorption experiments, with monitoring by FTIR spectroscopy, were conducted without exposure to air. Prior to adsorption experiments, the obtained sample was treated under O_2 at 600 °C to remove NO adsorbed during atomic dispersion reactions. The physical mixture of Pd black and CHA zeolite (Pd+CHA) was obtained by mixing commercially available Pd black (Nakalai Tesque, Ltd.) and CHA zeolite in gate mortar. The *in situ* XAS measurement was conducted on a flow-type quartz cell with a gas mixing system in a BL14B2, SPring-8 (JASRI, Proposal No. 2019B1686). *In situ* DRIFTS was performed using a FTIR spectrometer equipped with a diffuse reflectance cell. DFT calculations were performed with a periodic boundary condition under the Kohn−Sham formulation with the Vienna ab initio simulation package (VASP).[50,51] The generalized gradient approximated Perdew−Burke−Ernzerhof (GGA-PBE) functional was applied for electron exchange-correlation. XANES spectra were simulated for the DFT-optimized structures using the FDMNES software.[52,53] More detail on the experimental methodology is described in the Supporting Information (SI).

3. RESULTS AND DISCUSSION

3.1. Atomic Dispersion of Bulk Pd in Pd-Modified CHA Prepared by Impregnation Methods

The XRD pattern of Pd_{imp}/CHA (Pd: 5.4 wt %) exhibited typical diffraction patterns of CHA zeolite with a peak derived from PdO (101) at 2θ = 33.7° (Figure 1a). The FTIR spectrum from the CO adsorption experiment showed peaks resulting from stretching vibrations of C═O (ν(C═O)) from CO-coordinated Pd cations, such as $Pd^{2+}(CO)_2$, $Pd^{2+}(CO)$,

https://dx.doi.org/10.1021/jacsau.0c00112
JACS Au 2021, 1, 201−211

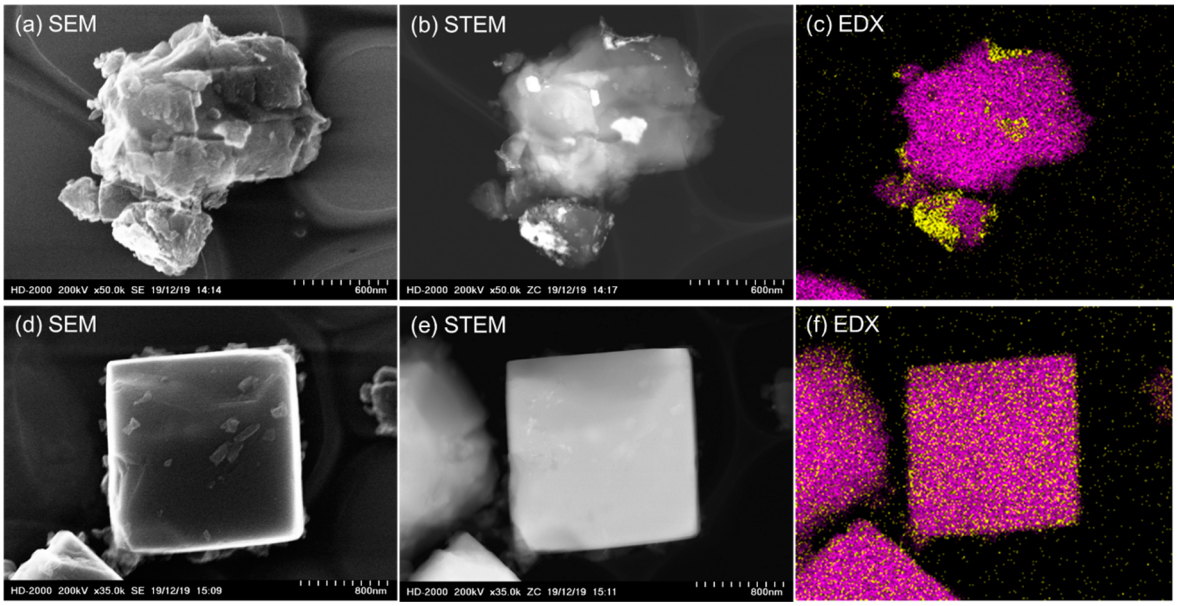

Figure 2. SEM (a and d), high-angle annular dark field STEM images (b and e), and elemental mapping of Pd (yellow) and Si (purple), obtained by EDX spectroscopy (c and f), for Pd_{imp}/CHA (a–c) and Pd_{imp}/CHA(H_2_NO) (d–f).

and $Pd^{+}(CO)$, around 2220–2100 cm^{-1} (Figure 1b).[54] Note that the group of Szanyi has recently revealed that the main two peaks around 2200 cm^{-1}, which had been assigned as $Pd^{3+}(CO)_2$,[22,55] are derived from highly positive $Pd^{2+}(CO)_2$ ions by experimental and theoretical approaches.[54,56] XRD and FTIR spectroscopy from the CO adsorption experiment indicated that both bulk PdO and atomic Pd cations exist after impregnation and calcination. The coexistence of bulk PdO and atomic Pd cations is further supported by SEM and STEM results, as well as energy dispersed X-ray (EDX) spectroscopy (Figure 2a–c).

To investigate the atomic dispersion of bulk Pd on the outside of CHA zeolite under oxidative conditions, Pd_{imp}/CHA was pretreated with 0.5% H_2/He at 500 °C for 30 min and, then, exposed to 4% NO/He flow at 600 °C for 30 min (Pd_{imp}/CHA(H_2_NO)). In the XRD pattern of Pd_{imp}/CHA(H_2_NO), the peak intensity derived from PdO (101) considerably decreased, while the diffraction pattern of CHA zeolite was retained (Figure 1a, the enlarged view (Figure S1) is shown in the SI). The FTIR spectrum collected from the CO adsorption experiment showed that absorptions derived from CO coordinated to Pd cations increased and peaks derived from CO adsorbed on the metallic Pd surface were scarce (Figure 1b). STEM and EDX spectroscopy (Figure 2d–f) showed the absence of aggregated Pd species. Together, these results suggest that the outside of bulk Pd was atomically dispersed into CHA zeolite by H_2 and NO treatment.

FTIR spectroscopy of the NO adsorption experiment was further conducted. One NO molecule is known to adsorb on one Pd^{n+} cation in zeolites, which exhibits a strong ν(N–O) absorption band around 1800–1900 cm^{-1}. We estimated the amount of NO adsorbed based on peak areas with the absorption coefficient value (see SI) and, then, calculated the molar ratio of adsorbed NO and total Pd in the samples (hereinafter denoted as NO/Pd, theoretical maximum is 100%) as an index of Pd dispersion. Prior to NO adsorption, the background spectrum was obtained after the 10% O_2/He treatment at 600 °C, followed by the He purge at 100 °C. The adsorption experiment was conducted under 0.1% NO/He flow at 100 °C, while continuously recording IR spectra. The IR spectra for Pd_{imp}/CHA and Pd_{imp}/CHA(H_2_NO) (Figure 1c) showed strong peaks at 1861 cm^{-1}, arising from ν(N–O) of $Pd^{2+}(NO)$, with shoulder peaks around 1810 cm^{-1}, assignable to $Pd^{+}(NO)$.[40] Note that the assignment of NO was well supported by the DFT studies in the previous paper.[54] The absorbance for Pd_{imp}/CHA(H_2_NO) was much higher than for Pd_{imp}/CHA; NO/Pd increased from 32.6% to 76.1% following H_2 and NO treatment. The NO adsorption experiment showed that mainly Pd^{2+} cations formed. When Pd_{imp}/CHA was directly treated with NO without H_2 reduction (Pd_{imp}/CHA(NO)), NO/Pd was calculated to be 49.1%, which was lower compared to Pd_{imp}/CHA(H_2_NO). The metallic state is essential for efficient atomic dispersion of outside bulk Pd species into small-pore CHA zeolites.

The effect of loading amounts (1, 5.4, and 6.8 wt %) on Pd dispersion was also investigated (The FTIR spectra are shown in Figure S2 in the SI). NO/Pd values were nearly the same for 1 and 5.4 wt % (78.7% and 76.1%), while the increase in loading amount to 6.8 wt % resulted in a decrease of the NO/Pd value to 63.3%. Based on the loading amount (5.4 wt %) and NO/Pd value, the contribution of Pd^{2+} cations was calculated to be 4.1 wt %. Considering that one Pd^{2+} cation is anchored by paired Al sites, the required amount of Al sites to stabilize 4.1 wt % of Pd^{2+} cations are theoretically estimated to be 0.76 mmol/g, which is lower than 50% of the total Al content of CHA (SiO_2/Al_2O_3 = 13.7) (2.1 mmol/g). Therefore, we can consider that all the Pd cations exist on Al sites.

To support the formation of Pd cations in CHA zeolites, an *ex situ* XAS measurement was carried out. The normalized XAS spectrum of Pd_{imp}/CHA(H_2_NO) after O_2 treatment exhibited an absorption edge similar to that of PdO, rather than Pd black (Figure 3a). In the FT of the extended X-ray absorption fine structure (EXAFS) spectra of Pd_{imp}/CHA and O_2-treated Pd_{imp}/CHA(H_2_NO), the peak derived from the Pd–(O)–Pd shell drastically decreased in intensity by H_2 and NO treatment (Figure 3b). The coordination number of the Pd–O shell for O_2-treated Pd_{imp}/CHA(H_2_NO) was

https://dx.doi.org/10.1021/jacsau.0c00112
JACS Au 2021, 1, 201–211

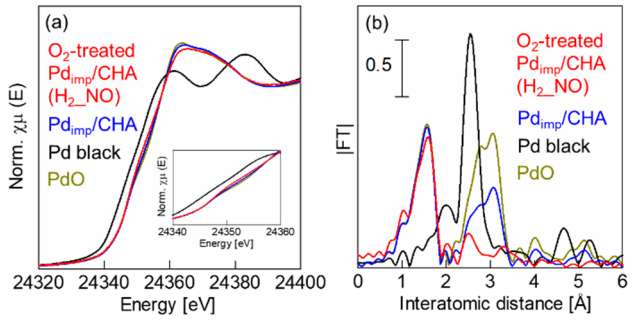

Figure 3. (a) *Ex situ* XANES and (b) FT of EXAFS spectra of Pd_{imp}/CHA, O_2-treated Pd_{imp}/CHA(H_2_NO), and reference samples (Pd Black and PdO) obtained under ambient conditions (air at room temperature).

estimated as 3.5 (Table S1). These results are consistent with the formation of Pd cations.

Furthermore, FTIR spectroscopy of NH_3 adsorption was conducted to investigate the coordination of Pd cations for the O_2-treated Pd_{imp}/CHA(H_2_NO) with different Pd loading amounts (1, 3, and 5.4 wt %). The spectrum of H−CHA after NH_3 adsorption exhibited a strong absorption band arising from NH_3 on protons at zeolite Al sites (Figure 4a).[57] The

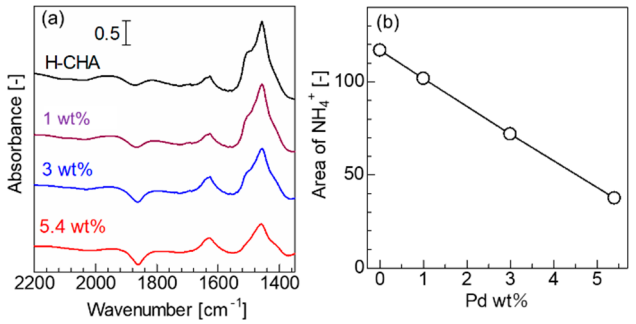

Figure 4. (a) FTIR spectra of NH_3 adsorption for H-CHA and O_2-treated Pd_{imp}/CHA(H_2_NO) with different Pd loading amounts (1, 3, and 5.4 wt %). The adsorption experiment was conducted at 50 °C under 1% NH_3/He flow, followed by a He purge. Prior to the adsorption experiments, the sample was treated by He flow at 600 °C. The detailed procedures are described in the SI. (b) Relationship between the peak area of the absorption band, derived from NH_4^+ and Pd loading amount.

peak area of this band monotonically decreased with increasing loading amounts from 1 to 5.4 wt % (Figure 4a and 4b), indicating Pd^{2+} cations were immobilized at Al sites in CHA zeolites. To support this consideration, SiO_2-supported Pd (Pd_{imp}/SiO_2, 5.4 wt %) was prepared and, then, treated with 0.5% H_2/He flow, followed by 4% NO/He treatment, in a similar manner. However, the NO adsorbed on atomic Pd cations was hardly detected, and NO/Pd was about 1% (Figure S3), showing that anchoring sites are necessary for atomic dispersion.

3.2. Preparation of Pd-Exchanged CHA from Pd Black and CHA Zeolites

Encouraged by the above results, we envisioned that NO-induced atomic dispersion of outside bulk Pd can be utilized for a physical mixture of Pd black and CHA zeolites (Pd +CHA, Pd: 5.4 wt %). This solid-state reaction would be another preparation method of Pd-exchanged CHA zeolites with high Pd cation loading amounts. Submicrosized bulk Pd and microsized cubic zeolites were observed by field-emission- and backscattered-electron SEM (FE- and BSE-SEM) and EDX mapping (Figure 5a). Pd+CHA was pretreated under 0.5% H_2/He flow at 300 °C, followed by treatment with 4% NO/He flow at 600 °C for 2 h (Pd+CHA(NO)). SEM micrographs with EDX mapping of Pd+CHA(NO) revealed that highly dispersed Pd species were immobilized in CHA zeolites, whereas submicrosized Pd species were hardly observed (Figure 5b). In the XRD spectra, the diffraction peak derived from Pd(111), around 2θ = ca. 40°, disappeared after NO treatment, while the diffraction pattern of CHA zeolite was maintained (Figure 6a).

Atomic dispersion of Pd black was evaluated by FTIR spectroscopy of CO and NO adsorption experiments for Pd +CHA and Pd+CHA(NO). The FTIR spectrum from the CO adsorption experiment revealed the formation of atomic Pd cations by NO treatment. The spectrum of NO adsorption showed that the NO/Pd value significantly increased from 9.9% to 76.3%. The results in the CO and NO adsorption experiments for Pd+CHA(NO) and Pd_{imp}/CHA(H_2_NO) are almost the same. As control experiments, O_2 and CO were used instead of NO for treatment of Pd+CHA (Pd+CHA(O_2) and Pd+CHA(CO)), and then, their Pd dispersions were evaluated by NO adsorption experiments. The resulting NO/Pd values were 21.4% and 15.4%, respectively. NO treatment was most effective for atomic dispersion of bulk Pd. The recent study on preparation of Pd-loaded CHA zeolites via modified ion-exchange method reported by Szanyi has achieved a complete atomic dispersion (NO/Pd = 100%) for 1−1.9 wt % of total Pd loading whereas the increase of Pd loading amount resulted in the decrease of atomic dispersion (NO/Pd = 90% and 70% for 3 and 5 wt % of Pd loading, respectively).[40] In our case using NO-facilitated atomic dispersion of Pd black, a comparable NO/Pd (76.1%) was obtained for 5.4 wt % of Pd loading although complete atomic dispersion was not achieved for lower Pd loading amount (NO/Pd = 91.2% and 89.5% for 1 and 3 wt % of Pd loading, respectively. See below). The literature comparison of loading amount of Pd^{2+} cations is summarized in Table S2 in the SI.

3.3. Atomic Dispersion of Bulk Pd into Other Zeolites with Different Framework Types

The dispersion of Pd nanoparticles (NPs) in zeolites under oxidative reaction conditions has been studied by several research groups.[21,22,32] Primet and co-workers first demonstrated the dispersion of small Pd NPs in zeolites to afford Pd^{2+} cations.[21] They prepared Pd^{2+}-exchanged Y zeolites by an aqueous phase ion exchange method followed by the reduction treatment by H_2, affording the 2 nm Pd(0) NPs occluded in the zeolites. Subsequently, the oxidative redispersion of Pd NPs in the zeolite cages was conducted by NO at room temperature. Bell and Okumura independently reported the redispersion of small Pd NPs in MFI zeolites obtained by the H_2 reduction of Pd^{2+}-exchanged MFI zeolites in similar manners.[22,32] The redispersion of aggregated Pd by NO treatment has also been extensively utilized in the industry for catalyst regeneration.[30] However, the oxidative dispersion of bulk Pd, such as commercially available Pd black, was not investigated in the aforementioned studies.

To investigate the effect of zeolite framework types and the difference of small Pd NPs and bulk Pd in atomic dispersion, the reaction of a physical mixture of Pd black (Pd: 1 wt %) and

https://dx.doi.org/10.1021/jacsau.0c00112
JACS Au 2021, 1, 201−211

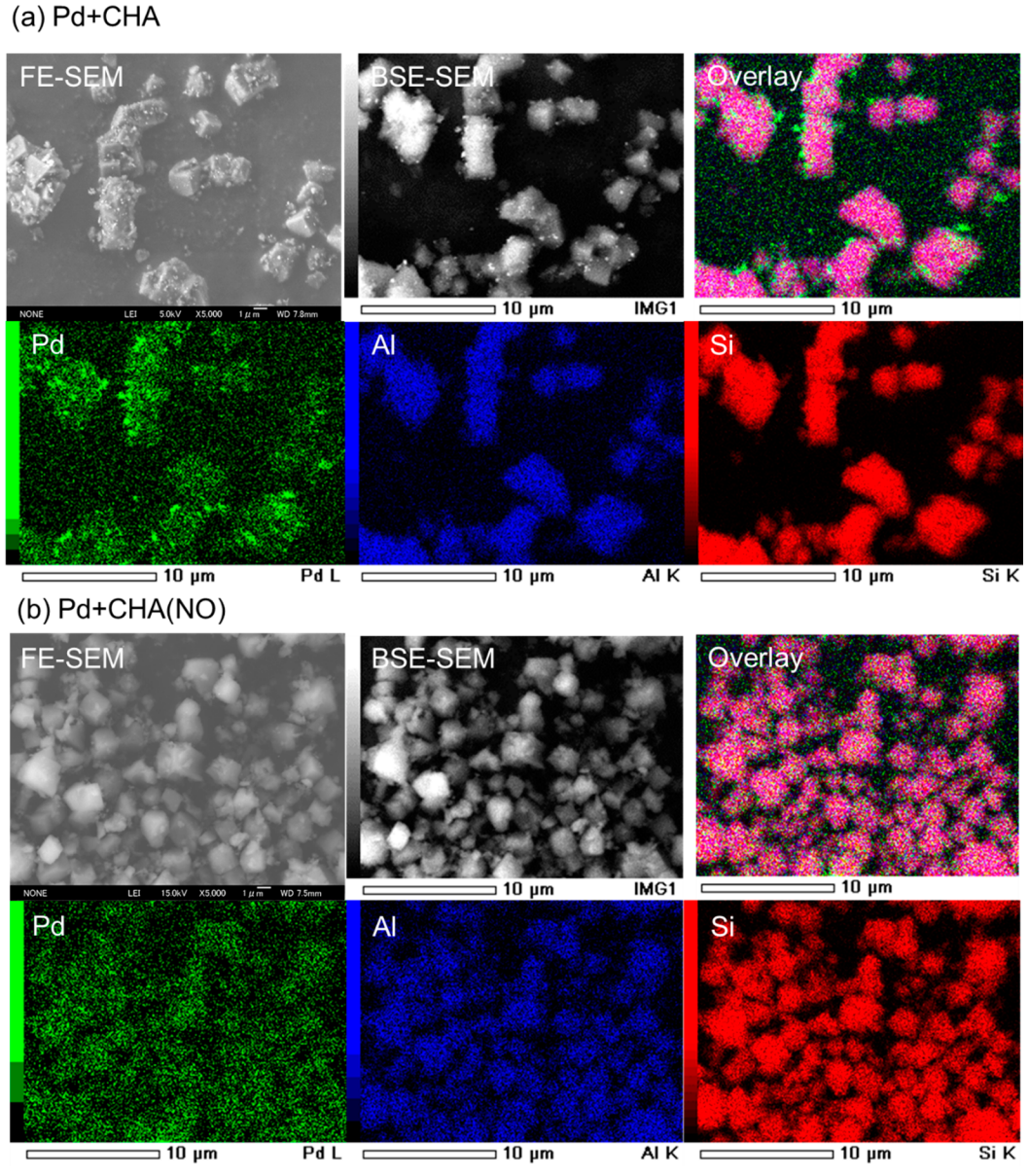

Figure 5. SEM images and elemental mapping of (a) Pd+CHA obtained by physical mixing of commercially available Pd black and CHA zeolites, and (b) Pd+CHA(NO) obtained by H_2 pretreatment and NO treatment of Pd+CHA.

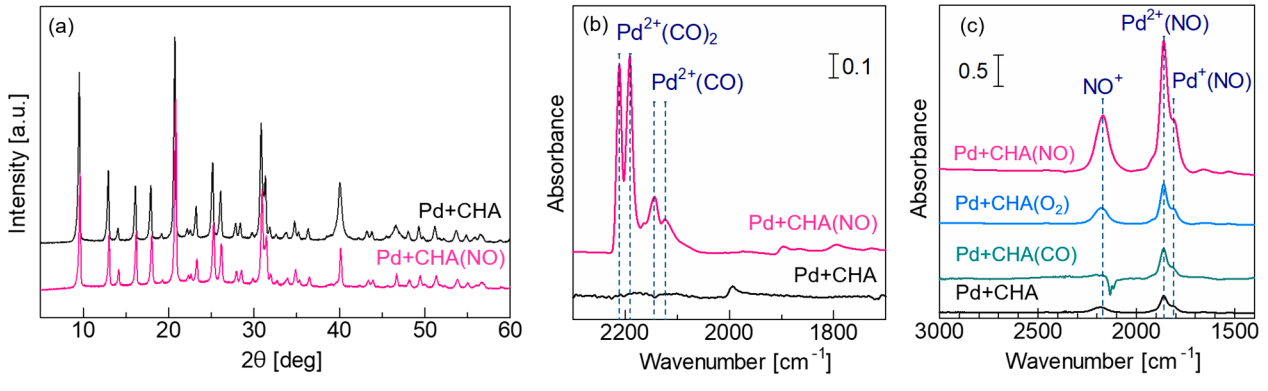

Figure 6. (a) XRD patterns and FTIR spectroscopy of (b) CO adsorption at room temperature and (c) NO adsorption at 100 °C for a series of Pd +CHA. Detailed procedures are described in the SI.

several zeolites, such as FER, MFI, MOR, BEA, and Y, with NO and then NO/Pd values were compared by NO adsorption experiment (Table 2). Note that Al contents in zeolites (0.9−3.2 mmol/g) are much higher than that required

https://dx.doi.org/10.1021/jacsau.0c00112
JACS Au 2021, 1, 201−211

Table 1. Comparison of NO/Pd Values Determined by NO Adsorption Experiments at 100 °C for a Series of Pd-Modified CHA or SiO_2 under Different Treatments[a]

Sample	Treatment	NO/Pd [%]	Pd cation[d] [wt %]
Pd_{imp}/CHA[b]	None	32.6	1.76
	H_2 followed by NO (30 min)	76.1	4.11
	NO (30 min)	49.1	2.65
Pd+CHA[b]	None	9.9	0.53
	NO (2 h)	76.3	4.12
	O_2 (2 h)	21.4	1.16
	CO (2 h)	15.4	0.83
Pd_{imp}/SiO_2[c]	None	1.7	0.09
	H_2 followed by NO (30 min)	1.5	0.08

[a]The details of NO adsorption experiments and adsorption coefficient are described in the SI. [b]Total Pd loading amount: 5.4 wt %. [c]Total Pd loading amount: 5.0 wt %. [d]Estimated from the total Pd loading amount and NO/Pd value.

Table 2. NO/Pd Values Determined by NO Adsorption Experiments at 100 °C for the Reaction of Physical Mixture of Pd Black and Other Zeolites with Different Framework Types under NO at 600 °C[a]

Zeolites	SAR[b]	Total Pd loading [wt %]	NO/Pd [%]	Pd cation[c] [wt %]
CHA	13.7	5.4	76.3	4.12
CHA	13.7	3.0	89.5	2.69
CHA	13.7	1.0	91.2	0.86
FER	18.0	1.0	93.4	0.93
MFI	22.3	1.0	93.7	0.94
MOR	20.0	1.0	73.0	0.73
BEA	17.5	1.0	48.9	0.49
Y	5.5	1.0	5.1	0.05

[a]The details of NO adsorption experiments and adsorption coefficient are described in the SI. [b]SiO_2/Al_2O_3 ratio. [c]Estimated from the total Pd loading amount and NO/Pd value.

to stabilize 1 wt % of Pd^{2+} cations (ca. 0.19 mmol/g) in all cases (The details are described in the SI). For FER, MFI, and MOR zeolites, high NO/Pd values were achieved (73.0–93.7%), while a moderate NO/Pd value was obtained in the case of BEA (48.9%). The use of Y zeolites resulted in an extremely low NO/Pd value (5.1%). These results showed that the present method utilizing atomic dispersion of bulk Pd was applicable to other zeolites tested (CHA, FER, MFI, MOR, and BEA) except for Y zeolites. In all the case, the XRD patterns obtained after the NO treatment showed that the diffraction peak derived from Pd(111) decreased in intensity (Figure S4), indicating that the reaction of bulk Pd with NO occurred for all the zeolites. Taking into account the report on redispersion of small Pd NPs by NO in Y zeolites at room temperature,[21] Y zeolites are unlikely to stabilize atomic Pd cations in high reaction temperature.

3.4. Spectroscopic and Theoretical Elucidation of Plausible Reaction in Atomic Dispersion of Bulk Pd into CHA Zeolites

All described results for Pd_{imp}/CHA, Pd+CHA, and Pd_{imp}/SiO_2 and those after different treatments (Table 1) clearly showed that (1) the reaction of Pd(0) metal with NO is a key and (2) Pd^{2+} cations are formed on zeolite Al sites. To elucidate the structural evolution of Pd species during atomic dispersion, an *in situ* XAS measurement was carried out for Pd+CHA during NO treatment (4% NO/He flow, 600 °C). Normalized XANES spectra obtained at t = 0, 2, 20, 60, 120, and 145 min are shown in Figure 7a. Prior to measurement Pd

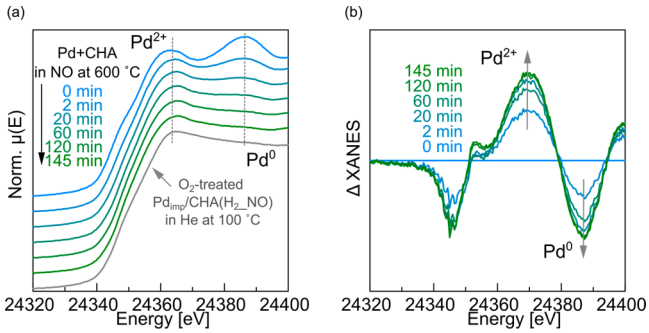

Figure 7. (a) *In situ* XANES spectra during the reaction of Pd+CHA under 4% NO/He flow at 600 °C and O_2-treated Pd_{imp}/CHA-(H_2_NO) under He flow at 100 °C. (b) Corresponding ΔXANES spectra. The data were obtained by subtraction with the spectrum taken at 0 min.

+CHA was treated with 0.5% H_2/He, followed by purging under He flow. The spectrum after pretreatment showed a peak unique to Pd(0) metal around 24388 eV with an absorption edge (E_0) at 24344.7 eV. When NO/He was introduced, the peak around 24388 eV decreased, with the concomitant appearance of a new peak derived from Pd^{2+} species around 24365 eV, while the absorption edge shifted toward higher energy. After 120 min of treatment with NO, the peak around 24388 eV disappeared, and the absorption edge remained unchanged (E_0 = 24349.0 eV). The XANES spectrum at 120 min resembled O_2-treated Pd_{imp}/CHA-(H_2_NO) under He flow at 100 °C, implying the formation of Pd^{2+} cations primarily. These changes are shown more clearly in the ΔXANES spectra (Figure 7b). The peak derived from Pd(0) species steeply decreased in intensity with the appearance of the peak assignable to Pd^{2+} species in the initial stage (t = 0–20 min) and, then, continuously decreased until t = 120 min. From these results, Pd black was atomically dispersed by oxidation of Pd(0) species toward Pd^{2+}.

In situ DRIFTS measurements were also conducted by monitoring the produced gas. The background spectrum was taken after pretreatment of Pd+CHA with H_2/He, followed by a He purge. After that, the gas was changed to 4% NO/He, while recording the spectra continuously. A negative band was observed around 3600 cm^{-1} upon exposure to NO, and its absorbance became more negative with extended treatment times (Figure 8a). This phenomenon can be ascribed to consumption of protons on Al sites (H^+ O_z^-) of CHA zeolites, owing to a cation-exchange reaction with Pd^{2+} cations. Further, NO adsorbed on *in situ* generated Pd^{2+} cations was detected. The gas product analysis revealed that N_2O was generated as a main gas product (Figure 8b). Plots of N_2O concentration and IR area for H^+ O_z^- versus time (Figure 8c) showed that N_2O formation and consumption of H^+ O_z^- occurred simultaneously. Combined with *in situ* XAS results, the atomic dispersion of bulk Pd can be described by the following equation (eq 1).

$$Pd(0) + 2NO + 2(H^+O_z^-) \rightarrow 2O_z^-Pd^{2+} + N_2O + H_2O \quad (1)$$

https://dx.doi.org/10.1021/jacsau.0c00112
JACS Au 2021, 1, 201–211

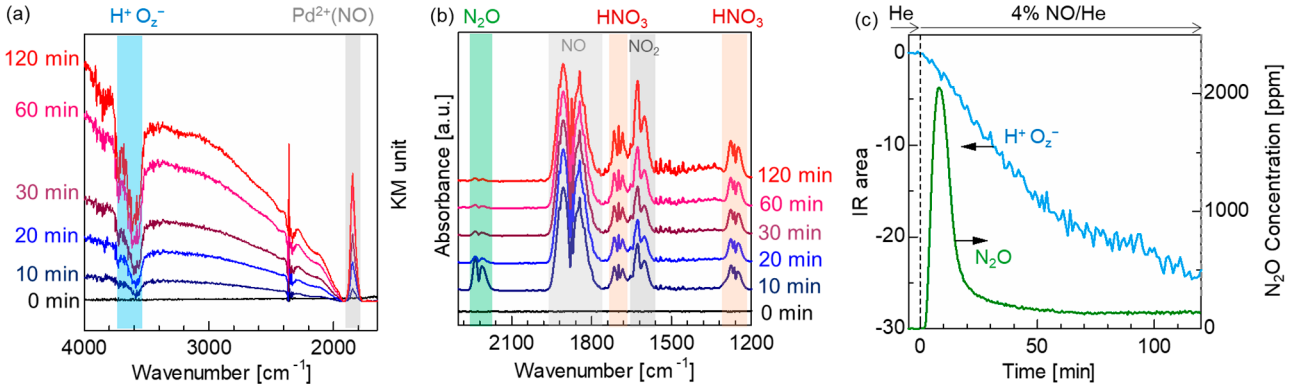

Figure 8. (a) *In situ* DRIFTS spectra during the reaction of Pd+CHA under 4% NO/He flow at 600 °C. (b) Spectra for NO_x gases monitored by IR with a gas cell. (c) Plots of N_2O concentration and IR area for H^+ O_z^-.

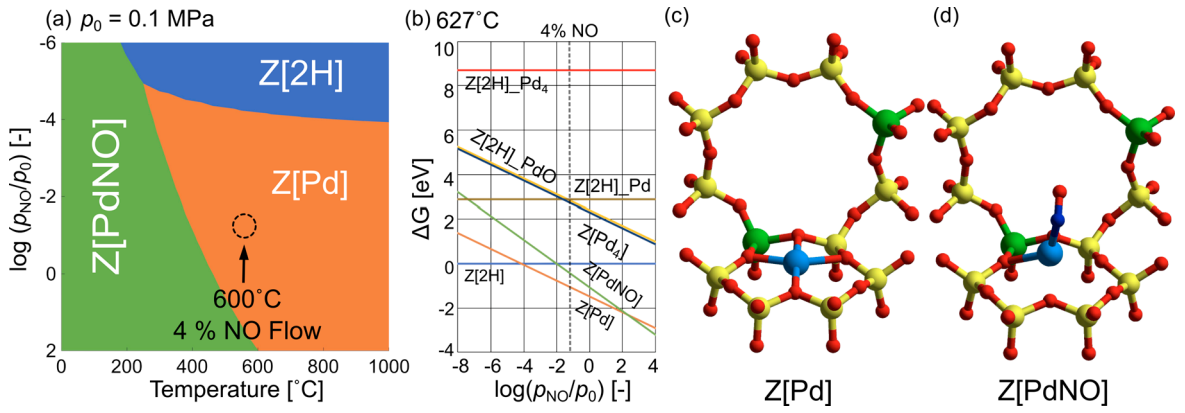

Figure 9. (a) Relative Gibbs free energy (ΔG) of the Pd species on paired Al sites (denoted as Z) in CHA zeolite, and a phase diagram showing the lowest-energy species as a function of NO partial pressure ($\log(p_{NO}/p_0)$) and temperature. (b) ΔG of Pd species on Z in CHA zeolite as a function of $\log(p_{NO}/p_0)$ at 627 °C. The optimized structures of (c) Z[Pd] and (d) Z[PdNO] are given. Yellow: Si, Red: O, Green: Al, Blue: N, Cyan: Pd. Only atoms around Z are shown for clarity.

A similar equation was proposed by Perimet and co-workers.[21] The amount of generated N_2O was estimated to be 328 μmol/g, which was ca. 65% of the total molar amount of Pd (508 μmol/g), supporting that the above equation (eq 1) is the most plausible reaction of atomic dispersion. However, HNO_3 was detected instead of H_2O. The generated H_2O may react with NO_2 derived from a decomposition reaction of NO under high temperature,[58] yielding HNO_3. Furthermore, atomic dispersion of bulk Pd in CHA zeolites was theoretically studied. Periodic DFT calculations, combined with *ab initio* thermodynamics analysis, were used to figure a phase diagram to predict plausible Pd species at relevant partial pressures and temperatures.[59,60] The following equilibrium reaction was considered (eq 2):

$$\begin{aligned} &\mathrm{Z[2H]} + n\mathrm{Pd_{bulk}} + (-x - y + 2z + 2)\mathrm{NO} \\ &\quad \rightleftharpoons \mathrm{Z[H_{x(0or2)}Pd_nN_yO_z]} + \left(-\frac{1}{2}x + 1\right)\mathrm{H_2O} \\ &\quad + \left(-\frac{1}{2}x - y + z + 1\right)\mathrm{N_2O} \end{aligned} \tag{2}$$

Paired Al sites possessing two O_z^- are denoted as Z. Detailed definitions for relative Gibbs free energies (ΔG) of $Z[H_{x(0or2)}Pd_nN_yO_z]$ and chemical potentials of gaseous molecules are described in the SI. The third-nearest-neighbor site in the eight-membered-ring is considered as Z, where the Al–Al distance is moderate (7.18 Å) among paired Al sites in CHA zeolite.[61] Proton-type CHA zeolite, in which two protons are possessed at Z for charge compensation, is treated as the reference model. This model is denoted as Z[2H], meaning that Pd species remain as bulk Pd. For divalent cationic species, a Pd^{2+} cation (Z[Pd]), NO-adsorbed Pd^{2+} cation (Z[PdNO]), and cationic Pd tetramer ($Z[Pd_4]$) are taken into account. A PdO monomer (Z[2H]_PdO), Pd atom (Z[2H]_Pd), and Pd tetramer ($Z[2H]\_Pd_4$) are evaluated as uncoordinated neutral species. Note that $Z[Pd_4]$ and $Z[2H]\_Pd_4$ have been applied as representative models of small Pd clusters in previous papers.[62,63] The structural information (CONTCAR files) of all the considered structures can be found in the SI. Note that the simulated XANES spectrum for the optimized Z[Pd] structure is similar to the experimental one for $Pd_{imp}/CHA(H_2\_NO)$ (Figure S5), confirming that our model is reasonable as Pd^{2+} cations in CHA zeolites.

Figure 9a shows the phase diagram as a function of partial pressure of NO ($\log(p_{NO}/p_0)$) and temperature. Z[PdNO] (Figure 9c) is the lowest species in free energy over a wide range of lower temperature conditions (<300 °C). With an increase of temperature at $\log(p_{NO}/p_0) > -4$, Z[Pd] (Figure 9d) becomes the most stable Pd species, while Z[2H] is predicted as the most stable structure under low NO concentrations in the high-temperature region. Figure 9b shows the calculated ΔG as a function of $\log(p_{NO}/p_0)$ at 627 °C. In the lower concentration region, ΔG values, for all considered Pd species, are higher than for Z[2H]. With

https://dx.doi.org/10.1021/jacsau.0c00112
JACS Au 2021, 1, 201–211

increasing NO concentration, ΔG for Z[PdNO], Z[Pd], Z[2H]_PdO, and Z[Pd_4] decrease. At $\log(p_{NO}/p_0) = -1.4$, corresponding to experimental conditions employed in this study (4% NO/He), Z[PdNO] and Z[Pd] are thermodynamically more favorable than Z[2H].

To confirm the requirement of high temperature for atomic dispersion of bulk Pd, the physical mixture of Pd black (5.4 wt %) with CHA zeolites was treated by NO at different temperatures from 30−600 °C. The results are summarized in Figure S6 and Table S3 in the SI. The atomic dispersion scarcely occurred at room temperature even by extending the time to 48 h (NO/Pd < 1%), and 600 °C was required to obtain high NO/Pd values (76.3%). Furthermore, the reason for the necessity of high temperature was theoretically studied. Several previous studies on atomic dispersion of Pd NPs under oxidative conditions proposed that the formation of mononuclear Pd species, including PdO,[21] $Pd(OH)_2$,[35] and Pd-nitrosyl complexes,[64] play key roles for the dispersion. In our experiments for the atomic dispersion of Pd black into CHA zeolites, the use of O_2 instead of NO induced the formation of bulk PdO, as indicated by XRD (Figure S7), and resulted in the significant decrease of Pd^{2+} cations (Table 1) while any mobile Pd-nitrosyl complex was not detected during the dispersion process using NO unfortunately (confirmed by FTIR). Therefore, the formation of mononuclear PdO from partially oxidized Pd surfaces was considered as a simple calculation model to discuss the difference between bulk Pd and Pd NPs in NO-induced atomic dispersion. A Pd(111) surface slab and a Pd_{38} cluster[65] with surface atomic O species were applied as representative models for Pd bulk surface and Pd NPs, respectively, and the formation energy of PdO vacancy (E_{PdOvac}) was compared (the used models and detailed definition can be found in the SI). The E_{PdOvac} for the Pd(111) surface is highly endothermic (168.7 kJ/mol) while that for the Pd_{38} cluster is relatively small (4.3 kJ/mol) (Figure S8a). Furthermore, the diffusion of generated PdO species in CHA zeolite pores was also investigated by transition state calculation, resulting in the small diffusion barrier through the eight-membered ring (28.3 kJ/mol, Figure S8b).[66] Considering the previous studies on reaction of metallic Pd with NO,[67,68] a plausible mechanism can be proposed as follows. A surface Pd atom is oxidized by the atomic O species generated by the dissociation of a NO molecule on a Pd metal surface.[67] A N_2O molecule is concomitantly generated from the remaining N and another NO.[68] Subsequently, a mononuclear PdO is formed from the oxidized Pd surface. This step is highly endothermic and thus requires high temperature. The generated PdO species can easily diffuse and access paired Al sites in CHA zeolites, and finally isolated Pd^{2+} cations are placed at ion-exchange sites with concomitant formation of H_2O. The paired Al sites in CHA zeolites can serve as anchoring sites of Pd^{2+} cations even under high reaction temperature, enabling NO-facilitated atomic dispersion of bulk Pd.

4. CONCLUSIONS

We have shown that bulk Pd can be atomically dispersed into small pores of CHA zeolite with 4% NO flow at 600 °C. The microscopic (SEM, STEM, EDX) and spectroscopic (XRD, FTIR, XAS) characterizations showed that Pd^{2+} cations on zeolite anionic sites were mainly formed. The amount of Pd^{2+} cations reached 4.1 wt %, which is higher than the highest value reported previously. The solid-state synthesis of Pd-exchanged CHA from commercially available Pd black and CHA zeolites was also demonstrated, where NO was the most effective among other reactive gases tested, such as O_2 and CO. The present method utilizing atomic dispersion of Pd black was applicable to other zeolites with different framework types. From *in situ* XAS and DRIFTS, combined with online gas monitoring, atomic dispersion occurs through oxidation of Pd metal by NO, yielding Pd cations on Al sites with concomitant formation of N_2O and H_2O (as HNO_3). The phase diagram, determined by *ab initio* thermodynamics analysis, showed that divalent Pd cations on paired Al sites are thermodynamically favored under the experimental conditions (4% NO and 600 °C), consistent with the occurrence of atomic dispersion of bulk Pd. The DFT calculations suggest that the generation of mononuclear Pd species from bulk Pd is a highly endothermic reaction and thus requires high reaction temperature. The generated mononuclear Pd species can easily diffuse into small-pore CHA zeolites to afford Pd^{2+} cations on paired Al sites. The paired Al sites in CHA zeolites stabilize atomic Pd cations even under severe reaction conditions, allowing the preparation of Pd^{2+}-loaded CHA zeolites from commercially available Pd black and CHA zeolites. This work demonstrates the potential of atomic dispersion for preparation of metal cation-exchanged small-pore zeolites that cannot be obtained by conventional aqueous-phase cation-exchange methods. It is noteworthy that the present method can be combined with the conventional methods. The NO adsorption/desorption properties and hydrothermal stability of Pd-loaded CHA zeolites with high loading of Pd^{2+} cations are now under investigation for PNA applications.

■ ASSOCIATED CONTENT

Supporting Information

The Supporting Information is available free of charge at https://pubs.acs.org/doi/10.1021/jacsau.0c00112.

Detailed procedures and results of experiments and calculations (PDF)

Complete structure files for the calculated structures (ZIP)

■ AUTHOR INFORMATION

Corresponding Authors

Zen Maeno − *Institute for Catalysis, Hokkaido University, Sapporo 001-0021, Japan;* orcid.org/0000-0002-9300-219X; Email: maeno@cat.hokudai.ac.jp

Ken-ichi Shimizu − *Institute for Catalysis, Hokkaido University, Sapporo 001-0021, Japan; Elements Strategy Initiative for Catalysts and Batteries, Kyoto University, Katsura, Kyoto 615-8520, Japan;* orcid.org/0000-0003-0501-0294; Email: kshimizu@cat.hokudai.ac.jp

Authors

Shunsaku Yasumura − *Institute for Catalysis, Hokkaido University, Sapporo 001-0021, Japan*

Hajime Ide − *Institute for Catalysis, Hokkaido University, Sapporo 001-0021, Japan*

Taihei Ueda − *Institute for Catalysis, Hokkaido University, Sapporo 001-0021, Japan*

Yuan Jing − *Institute for Catalysis, Hokkaido University, Sapporo 001-0021, Japan*

https://dx.doi.org/10.1021/jacsau.0c00112
JACS Au 2021, 1, 201−211

Chong Liu − *Institute for Catalysis, Hokkaido University, Sapporo 001-0021, Japan;* orcid.org/0000-0003-0311-8744

Kenichi Kon − *Institute for Catalysis, Hokkaido University, Sapporo 001-0021, Japan*

Takashi Toyao − *Institute for Catalysis, Hokkaido University, Sapporo 001-0021, Japan; Elements Strategy Initiative for Catalysts and Batteries, Kyoto University, Katsura, Kyoto 615-8520, Japan;* orcid.org/0000-0002-6062-5622

Complete contact information is available at: https://pubs.acs.org/10.1021/jacsau.0c00112

Author Contributions

S.Y. performed the atomic dispersion experiments, *in situ* DRIFTS measurements, and DFT calculations and wrote the draft. H.I. examined the NO/CO adsorption experiments as well as XRD and SEM measurements. T.U. conducted the NH_3 adsorption experiments and *ab initio* thermodynamics analysis. J.Y. performed *in situ* XAS measurements and analyzed the data. K.K. performed SEM, STEM, and EDX observations. C.L., T.T., and Z.M. critically revised the manuscript. K.S. designed and supervised the whole project.

Notes

The authors declare no competing financial interest.

■ ACKNOWLEDGMENTS

This study was financially supported by KAKENHI (Grant Nos. No. 17H01341, 20H02518, and 20H02775) from the Japan Society for the Promotion of Science (JSPS) and by the Japanese Ministry of Education, Culture, Sports, Science, and Technology (MEXT) within the projects "Integrated Research Consortium on Chemical Sciences (IRCCS)" and "Elements Strategy Initiative to Form Core Research Center" (JPMXP0112101003). This study was also supported by the JST-CREST projects JPMJCR17J3 and JPMJCR15P4. C.L. acknowledges a JSPS postdoctoral fellowship (No. P19059). The authors sincerely thank the technical division of the Institute for Catalysis (Hokkaido University) for manufacturing experimental equipment as well as the technical staff at the Open Facility of Hokkaido University for their assistance with STEM observations. X-ray absorption measurements were performed at the BL14B2 facilities of SPring-8 at the Japan Synchrotron Radiation Research Institute (JASRI) (No. 2019B1686). Part of the calculations were conducted on supercomputers at RIIT (Kyushu Univ.).

■ REFERENCES

(1) Liu, L.; Corma, A. Metal Catalysts for Heterogeneous Catalysis: From Single Atoms to Nanoclusters and Nanoparticles. *Chem. Rev.* **2018**, *118*, 4981−5079.

(2) Mee, S. J. Supported Metals in Catalysis Edited by James A. Anderson and Marcos Fernandez Garcia. *Chem. Ind. (Chichester, United Kingdom)* **2013**, *77*, 47.

(3) Choi, S.; Drese, J. H.; Jones, C. W. Adsorbent Materials for Carbon Dioxide Capture from Large Anthropogenic Point Sources. *ChemSusChem* **2009**, *2*, 796−854.

(4) Wang, S.; Peng, Y. Natural Zeolites as Effective Adsorbents in Water and Wastewater Treatment. *Chem. Eng. J.* **2010**, *156*, 11−24.

(5) Liu, L.; Corma, A. Evolution of Isolated Atoms and Clusters in Catalysis. *Trends Chem.* **2020**, *2*, 383−400.

(6) Goodman, E. D.; Schwalbe, J. A.; Cargnello, M. Mechanistic Understanding and the Rational Design of Sinter-Resistant Heterogeneous Catalysts. *ACS Catal.* **2017**, *7*, 7156−7173.

(7) Simonsen, S. B.; Chorkendorff, I.; Dahl, S.; Skoglundh, M.; Sehested, J.; Helveg, S. Ostwald Ripening in a Pt/SiO_2 Model Catalyst Studied by In Situ TEM. *J. Catal.* **2011**, *281*, 147−155.

(8) Matos, J.; Ono, L. K.; Behafarid, F.; Croy, J. R.; Mostafa, S.; Delariva, A. T.; Datye, A. K.; Frenkel, A. I.; Roldan Cuenya, B. In Situ Coarsening Study of Inverse Micelle-Prepared Pt Nanoparticles Supported on γ-Al_2O_3: Pretreatment and Environmental Effects. *Phys. Chem. Chem. Phys.* **2012**, *14*, 11457−11467.

(9) DeRita, L.; Resasco, J.; Dai, S.; Boubnov, A.; Thang, H. V.; Hoffman, A. S.; Ro, I.; Graham, G. W.; Bare, S. R.; Pacchioni, G.; Pan, X.; Christopher, P. Structural Evolution of Atomically Dispersed Pt Catalysts Dictates Reactivity. *Nat. Mater.* **2019**, *18*, 746−751.

(10) Gänzler, A. M.; Casapu, M.; Vernoux, P.; Loridant, S.; Cadete Santos Aires, F. J.; Epicier, T.; Betz, B.; Hoyer, R.; Grunwaldt, J.-D. Tuning the Structure of Platinum Particles on Ceria In Situ for Enhancing the Catalytic Performance of Exhaust Gas Catalysts. *Angew. Chem., Int. Ed.* **2017**, *56*, 13078−13082.

(11) Hill, A. J.; Seo, C. Y.; Chen, X.; Bhat, A.; Fisher, G. B.; Lenert, A.; Schwank, J. W. Thermally Induced Restructuring of $Pd@CeO_2$ and $Pd@SiO_2$ Nanoparticles as a Strategy for Enhancing Low-Temperature Catalytic Activity. *ACS Catal.* **2020**, *10*, 1731−1741.

(12) Lee, H.; Habas, S. E.; Kweskin, S.; Butcher, D.; Somorjai, G. A.; Yang, P. Morphological Control of Catalytically Active Platinum Nanocrystals. *Angew. Chem., Int. Ed.* **2006**, *45*, 7824−7828.

(13) Hansen, T. W.; DeLaRiva, A. T.; Challa, S. R.; Datye, A. K. Sintering of Catalytic Nanoparticles: Particle Migration or Ostwald Ripening? *Acc. Chem. Res.* **2013**, *46*, 1720−1730.

(14) Aitbekova, A.; Wu, L.; Wrasman, C. J.; Boubnov, A.; Hoffman, A. S.; Goodman, E. D.; Bare, S. R.; Cargnello, M. Low-Temperature Restructuring of CeO_2-Supported Ru Nanoparticles Determines Selectivity in CO_2 Catalytic Reduction. *J. Am. Chem. Soc.* **2018**, *140*, 13736−13745.

(15) Ferré, G.; Aouine, M.; Bosselet, F.; Burel, L.; Cadete Santos Aires, F. J.; Geantet, C.; Ntais, S.; Maurer, F.; Casapu, M.; Grunwaldt, J. D.; Epicier, T.; Loridant, S.; Vernoux, P. Exploiting the Dynamic Properties of Pt on Ceria for Low-Temperature CO Oxidation. *Catal. Sci. Technol.* **2020**, *10*, 3904−3917.

(16) Nagai, Y.; Dohmae, K.; Ikeda, Y.; Takagi, N.; Tanabe, T.; Hara, N.; Guilera, G.; Pascarelli, S.; Newton, M. A.; Kuno, O.; Jiang, H.; Shinjoh, H.; Matsumoto, S. In Situ Redispersion of Platinum Autoexhaust Catalysts: An on-Line Approach to Increasing Catalyst Lifetimes? *Angew. Chem., Int. Ed.* **2008**, *47*, 9303−9306.

(17) Piccolo, L. Restructuring Effects of the Chemical Environment in Metal Nanocatalysis and Single-Atom Catalysis. *Catal. Today* **2020**, in press. DOI: 10.1016/j.cattod.2020.03.052

(18) Delariva, A. T.; Hansen, T. W.; Challa, S. R.; Datye, A. K. In Situ Transmission Electron Microscopy of Catalyst Sintering. *J. Catal.* **2013**, *308*, 291−305.

(19) Newton, M. A.; Belver-Coldeira, C.; Martínez-Arias, A.; Fernández-García, M. Dynamic In Situ Observation of Rapid Size and Shape Change of Supported Pd Nanoparticles during CO/NO Cycling. *Nat. Mater.* **2007**, *6*, 528−532.

(20) Simonsen, S. B.; Chorkendorff, I.; Dahl, S.; Skoglundh, M.; Sehested, J.; Helveg, S. Direct Observations of Oxygen-Induced Platinum Nanoparticle Ripening Studied by In Situ TEM. *J. Am. Chem. Soc.* **2010**, *132*, 7968−7975.

(21) Che, M.; Dutel, J. F.; Gallezot, P.; Primet, M. A Study of the Chemisorption of Nitric Oxide on PdY Zeolite. Evidence for a Room Temperature Oxidative Dissolution of Pd Crystallites. *J. Phys. Chem.* **1976**, *80*, 2371−2381.

(22) Aylor, A. W.; Lobree, L. J.; Reimer, J. A.; Bell, A. T. Investigations of the Dispersion of Pd in H-ZSM-5. *J. Catal.* **1997**, *172*, 453−462.

(23) Feng, S.; Song, X.; Liu, Y.; Lin, X.; Yan, L.; Liu, S.; Dong, W.; Yang, X.; Jiang, Z.; Ding, Y. In Situ Formation of Mononuclear Complexes by Reaction-Induced Atomic Dispersion of Supported Noble Metal Nanoparticles. *Nat. Commun.* **2019**, *10*, 5281.

(24) Jones, J.; Xiong, H.; DeLaRiva, A. T.; Peterson, E. J.; Pham, H.; Challa, S. R.; Qi, G.; Oh, S.; Wiebenga, M. H.; Hernández, X. I. P.;

Wamg, Y.; Datye, A. K. Thermally Stable Single-Atom Platinum-on-Ceria Catalysts via Atom Trapping. *Science* **2016**, *353*, 150−154.
(25) Moliner, M.; Gabay, J.; Kliewer, C.; Serna, P.; Corma, A. Trapping of Metal Atoms and Metal Clusters by Chabazite under Severe Redox Stress. *ACS Catal.* **2018**, *8*, 9520−9528.
(26) Maeno, Z.; Yasumura, S.; Wu, X.; Huang, M.; Liu, C.; Toyao, T.; Shimizu, K. Isolated Indium Hydrides in CHA Zeolites: Speciation and Catalysis for Nonoxidative Dehydrogenation of Ethane. *J. Am. Chem. Soc.* **2020**, *142*, 4820−4832.
(27) Sá, J.; Taylor, S. F. R.; Daly, H.; Goguet, A.; Tiruvalam, R.; He, Q.; Kiely, C. J.; Hutchings, G. J.; Hardacre, C. Redispersion of Gold Supported on Oxides. *ACS Catal.* **2012**, *2*, 552−560.
(28) Wei, S.; Li, A.; Liu, J. C.; Li, Z.; Chen, W.; Gong, Y.; Zhang, Q.; Cheong, W. C.; Wang, Y.; Zheng, L.; Xiao, H.; Chen, C.; Wamg, D.; Peng, Q.; Gu, L.; Han, X.; Li, J.; Li, Y. Direct Observation of Noble Metal Nanoparticles Transforming to Thermally Stable Single Atoms. *Nat. Nanotechnol.* **2018**, *13*, 856−861.
(29) Shwan, S.; Skoglundh, M.; Lundegaard, L. F.; Tiruvalam, R. R.; Janssens, T. V. W.; Carlsson, A.; Vennestrøm, P. N. R. Solid-State Ion-Exchange of Copper into Zeolites Facilitated by Ammonia at Low Temperature. *ACS Catal.* **2015**, *5*, 16−19.
(30) Huang, Y. Y.; LaPierre, R. B.; McHale, W. D. Process for Dispersing or Redispersing a Group VIII Noble Metal Species on a Porous Inorganic Support for Catalysts. EP306170A1, March 8, 1989.
(31) Apelian, M. R.; Fung, A. S.; Hatzikos, G. H.; Kennedy, C. R.; Lee, C. H.; Kiliany, T. R.; Ng, P. K.; Pappal, D. A. Regeneration of Noble Metal Containing Zeolite Catalysts via Partial Removal of Carbonaceous Deposits. US5393717A, February 28, 1995.
(32) Okumura, K.; Amano, J.; Yasunobu, N.; Niwa, M. X-Ray Absorption Fine Structure Study of the Formation of the Highly Dispersed PdO over ZSM-5 and the Structural Change of Pd Induced by Adsorption of NO. *J. Phys. Chem. B* **2000**, *104*, 1050−1057.
(33) Nishihata, Y.; Mizuki, J.; Akao, T.; Tanaka, H.; Uenishi, M.; Kimura, M.; Okamoto, T.; Hamada, N. Self-Regeneration of a Pd-Perovskite Catalyst for Automotive Emissions Control. *Nature* **2002**, *418*, 164−167.
(34) Paredis, K.; Ono, L. K.; Behafarid, F.; Zhang, Z.; Yang, J. C.; Frenkel, A. I.; Cuenya, B. R. Evolution of the Structure and Chemical State of Pd Nanoparticles during the In Situ Catalytic Reduction of NO with H_2. *J. Am. Chem. Soc.* **2011**, *133*, 13455−13464.
(35) Goodman, E. D.; Johnston-Peck, A. C.; Dietze, E. M.; Wrasman, C. J.; Hoffman, A. S.; Abild-Pedersen, F.; Bare, S. R.; Plessow, P. N.; Cargnello, M. Catalyst Deactivation via Decomposition into Single Atoms and the Role of Metal Loading. *Nat. Catal.* **2019**, *2*, 748−755.
(36) Jing, Y.; Cai, Z.; Liu, C.; Toyao, T.; Maeno, Z.; Asakura, H.; Hiwasa, S.; Nagaoka, S.; Kondoh, H.; Shimizu, K. Promotional Effect of La in the Three-Way Catalysis of La-Loaded Al_2O_3-Supported Pd Catalysts ($Pd/La/Al_2O_3$). *ACS Catal.* **2020**, *10*, 1010−1023.
(37) Yu, Q.; Chen, X.; Bhat, A.; Tang, X.; Yi, H.; Lin, X.; Schwank, J. W. Activation of Passive NOx Adsorbers by Pretreatment with Reaction Gas Mixture. *Chem. Eng. J.* **2020**, *399*, 125727.
(38) Ryou, Y. S.; Lee, J.; Lee, H.; Kim, C. H.; Kim, D. H. Effect of Various Activation Conditions on the Low Temperature NO Adsorption Performance of Pd/SSZ-13 Passive NOx Adsorber. *Catal. Today* **2019**, *320*, 175−180.
(39) Baba, T.; Komatsu, N.; Sawada, H.; Yamaguchi, Y.; Takahashi, T.; Sugisawa, H.; Ono, Y. O. 1H Magic Angle Spinning NMR Evidence for Dissociative Adsorption of Hydrogen on Ag^+-Exchanged A- and Y-Zeolites. *Langmuir* **1999**, *15*, 7894−7896.
(40) Khivantsev, K.; Jaegers, N. R.; Kovarik, L.; Hanson, J. C.; Tao, F.; Tang, Y.; Zhang, X.; Koleva, I. Z.; Aleksandrov, H. A.; Vayssilov, G. N.; Wang, Y.; Gao, F.; Szanyi, J. Achieving Atomic Dispersion of Highly Loaded Transition Metals in Small-Pore Zeolite SSZ-13: High-Capacity and High-Efficiency Low-Temperature CO and Passive NO_x Adsorbers. *Angew. Chem., Int. Ed.* **2018**, *57*, 16672−16677.
(41) Dusselier, M.; Davis, M. E. Small-Pore Zeolites: Synthesis and Catalysis. *Chem. Rev.* **2018**, *118*, 5265−5329.
(42) Beale, A. M.; Gao, F.; Lezcano-Gonzalez, I.; Peden, C. H. F.; Szanyi, J. Recent Advances in Automotive Catalysis for NO_x Emission Control by Small-Pore Microporous Materials. *Chem. Soc. Rev.* **2015**, *44*, 7371−7405.
(43) Schmieg, S. J.; Oh, S. H.; Kim, C. H.; Brown, D. B.; Lee, J. H.; Peden, C. H. F.; Kim, D. H. Thermal Durability of Cu-CHA NH_3-SCR Catalysts for Diesel NO_x Reduction. *Catal. Today* **2012**, *184*, 252−261.
(44) Deka, U.; Lezcano-Gonzalez, I.; Weckhuysen, B. M.; Beale, A. M. Local Environment and Nature of Cu Active Sites in Zeolite-Based Catalysts for the Selective Catalytic Reduction of NO_X. *ACS Catal.* **2013**, *3*, 413−427.
(45) Chen, H.-Y.; Mulla, S.; Weigert, E.; Camm, K.; Ballinger, T.; Cox, J.; Blakeman, P. Cold Start Concept (CSC^{TM}): A Novel Catalyst for Cold Start Emission Control. *SAE Int. J. Fuels Lubr.* **2013**, *6*, 372−381.
(46) Lee, J.; Theis, J. R.; Kyriakidou, E. A. Vehicle Emissions Trapping Materials: Successes, Challenges, and the Path Forward. *Appl. Catal., B* **2019**, *243*, 397−414.
(47) Khivantsev, K.; Jaegers, N. R.; Kovarik, L.; Prodinger, S.; Derewinski, M. A.; Wang, Y.; Gao, F.; Szanyi, J. Palladium/Beta Zeolite Passive NOx Adsorbers (PNA): Clarification of PNA Chemistry and the Effects of CO and Zeolite Crystallite Size on PNA Performance. *Appl. Catal., A* **2019**, *569*, 141−148.
(48) Zheng, Y.; Kovarik, L.; Engelhard, M. H.; Wang, Y.; Wang, Y.; Gao, F.; Szanyi, J. Low-Temperature Pd/Zeolite Passive NO_x Adsorbers: Structure, Performance, and Adsorption Chemistry. *J. Phys. Chem. C* **2017**, *121*, 15793−15803.
(49) Lee, H.; Song, I.; Jeon, S. W.; Kim, D. H. Inter-Particle Migration of Cu Ions in Physically Mixed Cu-SSZ-13 and H-SSZ-13 Treated by Hydrothermal Aging. *React. Chem. Eng.* **2019**, *4*, 1059−1066.
(50) Kresse, G.; Furthmüller, J. Efficiency of Ab-Initio Total Energy Calculations for Metals and Semiconductors Using a Plane-Wave Basis Set. *Comput. Mater. Sci.* **1996**, *6*, 15−50.
(51) Kresse, G.; Furthmüller, J. Efficient Iterative Schemes for Ab Initio Total-Energy Calculations Using a Plane-Wave Basis Set. *Phys. Rev. B: Condens. Matter Mater. Phys.* **1996**, *54*, 11169−11186.
(52) Joly, Y. X-Ray Absorption Near-Edge Structure Calculations beyond the Muffin-Tin Approximation. *Phys. Rev. B: Condens. Matter Mater. Phys.* **2001**, *63*, 125120.
(53) Bunău, O.; Joly, Y. Self-Consistent Aspects of X-Ray Absorption Calculations. *J. Phys.: Condens. Matter* **2009**, *21*, 345501.
(54) Khivantsev, K.; Jaegers, N. R.; Koleva, I. Z.; Aleksandrov, H. A.; Kovarik, L.; Engelhard, M.; Gao, F.; Wang, Y.; Vayssilov, G. N.; Szanyi, J. Stabilization of Super Electrophilic Pd^{2+} Cations in Small-Pore SSZ-13 Zeolite. *J. Phys. Chem. C* **2020**, *124*, 309.
(55) Chakarova, K.; Ivanova, E.; Hadjiivanov, K.; Klissurski, D.; Knözinger, H. Co-ordination Chemistry of Palladium Cations in Pd-H-ZSM-5 as Revealed by FTIR Spectra of Adsorbed and Co-Adsorbed Probe Molecules (CO and NO). *Phys. Chem. Chem. Phys.* **2004**, *6*, 3702−3709.
(56) Khivantsev, K.; Gao, F.; Kovarik, L.; Wang, Y.; Szanyi, J. Molecular Level Understanding of How Oxygen and Carbon Monoxide Improve NOx Storage in Palladium/SSZ-13 Passive NOx Adsorbers: The Role of NO^+ and Pd(II)(CO)(NO) Species. *J. Phys. Chem. C* **2018**, *122*, 10820−10827.
(57) Niwa, M.; Katada, N. Combined Method of Ammonia IRMS-TPD Experiment and DFT Calculation to Characterize Zeolite Acidity. *J. Jpn. Pet. Inst.* **2009**, *52*, 172−179.
(58) Yuan, E. L.; Slaughter, J. I.; Koerner, W. E.; Daniels, F. Kinetics of the Decomposition of Nitric Oxide in the Range 700−1800 °C. *J. Phys. Chem.* **1959**, *63*, 952−956.
(59) Reuter, K.; Scheffler, M. Composition, Structure, and Stability of $RuO_2(110)$ as a Function of Oxygen Pressure. *Phys. Rev. B: Condens. Matter Mater. Phys.* **2001**, *65*, No. 035406.
(60) Li, G.; Pidko, E. A.; van Santen, R. A.; Li, C.; Hensen, E. J. M. M. Stability of Extraframework Iron-Containing Complexes in ZSM-5 Zeolite. *J. Phys. Chem. C* **2013**, *117*, 413−426.

(61) Yasumura, S.; Huang, M.; Wu, X.; Liu, C.; Toyao, T.; Maeno, Z.; Shimizu, K. A CHA Zeolite Supported Ga-Oxo Cluster for Partial Oxidation of CH_4 at Room Temperature. *Catal. Today* **2020**, *352*, 118−126.
(62) Moc, J.; Musaev, D. G.; Morokuma, K. Zeolite-Supported Palladium Tetramer and Its Reactivity toward H_2 Molecules: Computational Studies. *J. Phys. Chem. A* **2008**, *112*, 5973−5983.
(63) Begum, P.; Gogoi, P.; Mishra, B. K.; Deka, R. C. Theoretical Insight of Nitric Oxide Adsorption on Neutral and Charged Pdn (n = 1−5) Clusters. *Int. J. Quantum Chem.* **2015**, *115*, 837−845.
(64) Goldsmith, B. R.; Sanderson, E. D.; Ouyang, R.; Li, W. X. CO- and NO-Induced Disintegration and Redispersion of Three-Way Catalysts Rhodium, Palladium, and Platinum: An Ab Initio Thermodynamics Study. *J. Phys. Chem. C* **2014**, *118*, 9588−9597.
(65) Posada-Borbón, A.; Heard, C. J.; Grönbeck, H. Cluster Size Effects in Ethylene Hydrogenation over Palladium. *J. Phys. Chem. C* **2017**, *121*, 10870−10875.
(66) Chen, L.; Jansson, J.; Skoglundh, M.; Grönbeck, H. Mechanism for Solid-State Ion Exchange of Cu^+ into Zeolites. *J. Phys. Chem. C* **2016**, *120*, 29182−29189.
(67) Loffreda, D.; Simon, D.; Sautet, P. Structure Sensitivity for NO Dissociation on Palladium and Rhodium Surfaces. *J. Catal.* **2003**, *213*, 211−225.
(68) Rainer, D. R.; Koranne, M.; Vesecky, S. M.; Goodman, D. W. $CO+O_2$ and CO+NO Reactions over Pd/Al_2O_3 Catalysts. *J. Phys. Chem. B* **1997**, *101*, 10769−10774.

https://dx.doi.org/10.1021/jacsau.0c00112
JACS Au 2021, 1, 201−211